Available online at www.sciencedirect.com

ScienceDirect

Energy Procedia 80 (2015) 245 – 254

Energy Procedia

12th Deep Sea Offshore Wind R&D Conference, EERA DeepWind'2015

Characterisation of single wind turbine wakes with static and scanning WINTWEX-W LiDAR data

Valerie-M. Kumer[a,b], Joachim Reuder[a,b], Benny Svardal[c], Camilla Sætre[c], Peter Eecen[d]

[a]Geophysical Institute, University of Bergen, Allegaten 70, 5007 Bergen, Norway
[b]Bjerknes Center for Climate Research, Allegaten 70, 5007 Bergen, Norway
[c]Christian Michelsen Research AS, Fantoftvegen 38, Bergen, Norway
[d]Energy research Centre of the Netherlands, Westerduinweg 3, Petten, The Netherlands

Abstract

With further development of LiDAR technology wake measurements by use of LiDAR became of common interest in the wind energy community. To study new measurement strategies of scanning and nacelle LiDARs, in combination with already existing measurement principles of static LiDARs, Norcowe conducted in collaboration with the Energy research Centre of the Netherlands (ECN) the Wind Turbine Wake Experiment Wieringermeer (WINTWEX-W). In this study we use data from the static Windcubes V1 to illustrate a proof of concept of wake effects at 1.75 and 3.25 rotor diameter downstream distance. After validating Windcube data against sonic anemometers from the met mast, we compare downstream velocity deficits and turbulence intensities between measurements of static and scanning WindCubes. To further characterize single wind turbine wakes and their frequencies of occurrence we analysed the results in terms of atmospheric stability. Wake measurements are of great importance to further developing tools for optimising wind farm layouts and operations.

Peer-review under responsibility of SINTEF Energi AS

Keywords: LiDAR, wind turbine wakes, planetary boundary layer, atmospheric stability

1. Introduction

The wake region of a wind turbine is in general characterized by a reduction in average wind speed and an increase in turbulence intensity. Both effects have negative implications for the operation of a wind farm by reducing the power output and increasing loads and fatigue for downstream turbines. The accurate characterization of the structure and dynamics of single turbine wakes is therefore the key for understanding the wind field inside a wind farm and of uttermost importance for wind farm designers and operators.

* Valerie-M. Kumer. Tel.: +47-55-58-2672.
E-mail address: valerie.kumer@gfi.uib.no

Peer-review under responsibility of SINTEF Energi AS
doi:10.1016/j.egypro.2015.11.428

Wakes are a complex interaction between the turbulent atmospheric boundary layer (ABL), the static structure of the turbine tower and the aerodynamics of the rotating turbine blades. In the past, wake effects have mainly been investigated by scaled wind tunnel studies (e.g. [1–4]) and model simulations of different complexity (e.g. [5], [6], [7], [8]). These approaches have contributed to a reasonable understanding of wind turbine wakes under idealized conditions, i.e. the assumption of neutral atmospheric stratification and corresponding use of a logarithmic wind profile. It is however evident that atmospheric stability plays an important role for the development, structure, dynamics and decay of wind turbine wakes ([9–13]) and that its' appropriate description requires corresponding long-term observations.

The recent development in the field of sodar(e.g. [14]), radar (e.g. [15]) and in particular lidar based remote sensing capabilities (e.g. [16] has opened new perspectives for such full scale wake observations under different atmospheric stability conditions. Static wind lidar systems, available for about one decade now, have been used to determine the average wake deficit in the wind profile behind a turbine (e.g. [17]) or to determine single volume turbulence statistics by operating the instruments in staring mode ([18,19]). With scanning wind lidars entering the market during the last years, the measurement capabilities related to structure and dynamics of turbine wakes have distinctly increased. However the corresponding campaigns have usually been limited to shorter measurement periods (e.g. [20–23]).

The presented study describes a 7 month multi-lidar deployment at the test site Wieringermeer operated by the Energy research Centre of the Netherlands (ECN). It combined 4 static wind lidar systems upstream and downstream of a row of test turbines with one scanning unit located around 12 rotor diameters downstream in the main wind direction. In addition 2 nacelle mounted horizontally looking lidars, operated part of the campaign one looking in the inflow and the other in the wake, and part of the campaign with both measuring the wake simultaneously. The main purpose of this campaign was to test a novel approach for the characterization of the structure and dynamics of single turbine wakes by the extensive use and combination of static and scanning wind lidar systems. The primary focus of this manuscript is the description of the campaign and the presentation of first results on the effects of atmospheric stability on the strength and extension of the wake downstream of single wind turbines.

2. Campaign Setup

Data used in this study origins from the WInd Turbine Wake EXperiment Wieringermeer (WINTWEX-W) conducted by the University of Bergen (UiB), Christian Michelsen Reserach (CMR) and the Energy research Centre of the Netherlands (ECN), all partners of the NORwegian Center of Offshore Wind Energy (NORCOWE). It took place from November 2013 until mid of May 2014 in ECN's Wind turbine test facilities in Wieringermeer, 1 km of the Wieringermeer coastline at -5 m below sea level, to test wake measurement of three different Doppler LiDAR instruments.

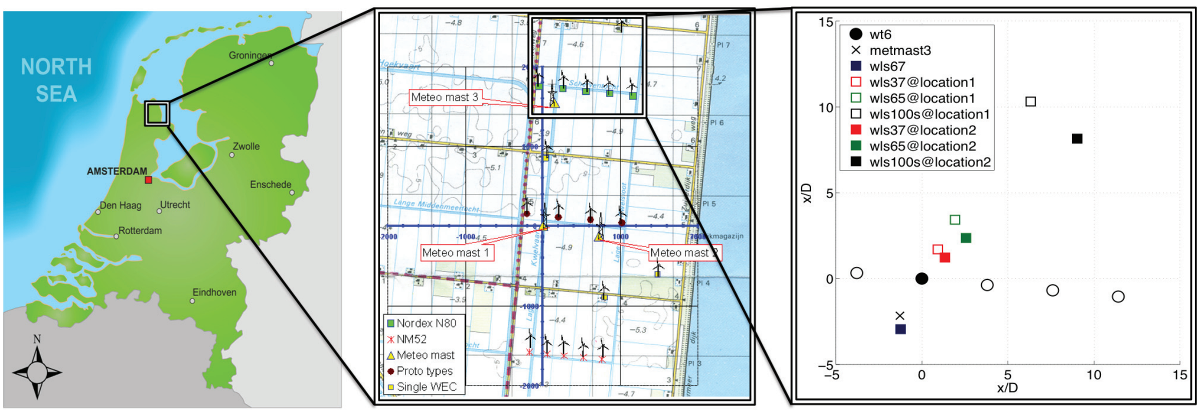

Fig. 1. a) Map of the Netherlands with a black box indicating the location of ECN's wind turbine test site Wieringermeer. b) Map of the wind turbine test site with a box indicating the row of research turbines. c) Map of the WINTWEX-W measurement setup around the research turbine number 6.

The test facility consists of a row of prototype turbines and a row of five Nordex 2.5 MW research wind turbines with a hub height and rotor diameter of 80 m. Around 3 rotor diameter upstream of the research turbine number 6 a met mast of 108 m measures upstream wind and temperature conditions at three and two different altitudes respectively (figure 1). In this study we use wind information of the 3D Gill Sonic at 80 and 108 m height and the temperature difference between 37 and 10 m. Additional to the standard met-mast instrumentation, we deployed one Windcube V1 upstream of the research turbine number 6 and two Windcube V1 and a Windcube 100s downstream. The downstream devices were located at 2, 5 and 12 rotor diameter distance aligned for winds coming from 210° degrees south-west. After relocation on November 29th 2013, the locations changed to 1.75, 3 and a 12 rotor diameter downstream along the wake line aligned for winds coming from 218° degrees south-west (figure 1). The Windcube V1s measured standard profiles at 40, 52, 60, 100, 108, 120, 140, 160, 200 m above ground level with a sampling frequency of 1 Hz. The scanning configuration of the Windcube 100s consisted of three Plan Position Indicator (PPI) and three Range Hight Indicator (RHI) scans repeating every minute (table 2).

scan type	azimuth [°]	elevation [°]	scan speed [°/*sec*]	scan duration [*sec*]
PPI	198 - 258	2.4	6	10
PPI	198 - 258	4.7	6	10
PPI	198 - 258	7.1	6	10
RHI	228	60 - 0	6	10
RHI	228	0 - 60	6	10
RHI	228	60 - 0	6	10

Table 1. Scan configuration of the Windcube 100S, consisting of three Plan Position Indicator (PPI) and three Range Hight Indicator (RHI) scans.

On the nacelle of the research turbine number 6 an upstream looking Wind Iris and a downstream looking Zephir (ZPH328) nacelle LiDAR also measured hub height up and downstream flow condition, but are not part of this study.

3. Data and Methods

The sonic and the upstream Windcube WLS67 data were available throughout the campaign duration. Due to the relocation and farm work the downstream Windcube WLS37 and WLS65 have some data gaps in end of November 2013 and from March until May 2014. For some days in December the daily average data availability at 108 m was below 50% (figure 2). Before relocation the downstream Windcube WLS37 had a directional offset form geographic north of 45°, which we corrected for the further analysis.

As a data quality control of the Windcube measurements we compared their ten minute mean wind speed and direction measurements to ten minute mean sonic measurements at 108 m height, which is located at the top of the upstream met-mast number 3. Following the data calibration recommend in the IEA Task 32 ([24]) we correlated the data according to wind speeds greater than $4ms^-1$, dry weather conditions, data availability greater than 90% and turbulence intensities smaller than 1%. Additionally, we highlighted correlations for undisturbed wind direction. Following correlation coefficients will refer to this undisturbed data. The first downstream Windcube (WLS37) was influenced by the wake of almost all research turbines. Therefore, only winds in the sectors between 150 to 210° and 250 to 260° were used for validation. For the second downstream Windcube we picked sectors between 330 to 20° and 100 to 310°. The upstream Windcube (WLS67) was validated against winds between 330 to 20° and 50 to 180°. Following Courtney ([25]), the Windcube 100s was validated not against the meteorological wind speeds measured by the sonic anemometer but against its converted radial wind speed component (equation 1) for all wind directions

$$vr_{sonic} = u * cos(\alpha) + v * sin(\alpha), \quad (1)$$

where u and v are the zonal and meridional wind components and α is the angle between geographic north and the line of sight measurement of the Windcube 100S that we choose for comparison. The collected data by the Windcubes V1 show a generally good quality with correlation coefficients varying between $R^2 = 0.946$ and $R^2 = 0.973$ for the horizontal wind speed and between $R^2 = 0.944$ and $R^2 = 0.998$ for the wind direction (figure 3). The ten minute mean radial wind speeds of the Windcube 100s, compare with a R^2 value of 0.645 not as good to the ten minute mean radial wind speeds of the sonic anemometer, which might be related to data processing issues. A comparison of horizontal

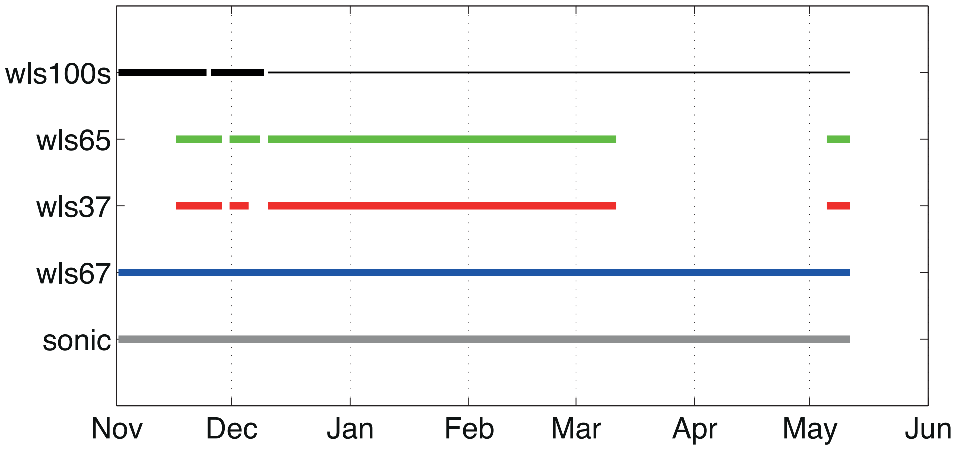

Fig. 2. Daily mean data availability greater than 50% at 108 m height of the sonic anemometer (grey), the Windcubes WLS67 (blue), WLS37 (red), WLS65 (green) and WLS100S (black).

wind speeds calculated from Windcube 100s measurements to Windcube V1 data by Hu show a higher correlation of $R^2 = 0.95$ ([26]).

The campaign was designed to study single wind turbine wakes. Therefore the downstream wind turbines were aligned in the main wind direction of south westerly winds (210 degrees) and only the sector around the main wind direction will be analysed to study wind turbine wake characteristics. Figure 4 shows the wind speed distribution of the analysed period from beginning of November 2013 until the mid of March 2014 at 108 m height, while highlighting the analysed wind sector. Narrowing the data to a 45 degree wind sector leaves us with 22 % of the analysed data set. 45 degrees were chosen over a smaller sector in order to increase the amount of data to allow for a more general conclusion. However, this leaves us with a more complex interpretation of the data inside the wake, since the Windcube profiles face wake position fluctuations.

The position of the Windcubes inside the wake are crucial for further interpretations of the data since, wake characteristics and measurement accuracies are different in the wake central line or at the edges ([27]). In order to print the average wake location in which the downstream Windcubes measured their profiles, a total average of each 10 second PPI scan was calculated. Additional to the wake characteristics at different positions the measurement principle of the profiling Windcubes is sensitive to complex flow. Wind vectors are retrieved by the Doppler Beam Swift (DBS) method using the last four radial wind speed measurements, assuming uniform flow. In non-uniform flow this assumption is broken and the measurement uncertainty of 0.5 m/s is expected to increase. However, measurement inter-comparisons by Rhodes et al. ([28]) and LES simulations of LiDAR measurements inside wake by Lundquist et al. ([27]) have shown that measurement errors will be ≤ 1 ms^{-1}. In order to analyse the profiles dependent on atmospheric stability, we put the data into three categories representing stable, unstable and neutral atmospheric states. A positive, non existent or a temperature gradient smaller than the dry adiabatic lapse rate was used to define stable, neutral and unstable conditions respectively.

4. Results

An analysis of the data shows a general proof of concept for both LiDAR measurement strategies. With the above described scan pattern we were able to catch single wind turbine wakes and some of their meandering characteristics (figure 5). An instantaneous PPI scan cutting though hub height shows a wave pattern with an increasing wave length downstream characterized by a band of radial velocity deficits of around 7 ms^{-1}, similar in magnitude to vertical scans by Iungo et al. ([20]). It is also interesting to see the signature of the upstream prototype turbine wakes with a much longer wave length and lower but still significant velocity deficits of around 4 ms^{-1}. On a 10 minutes average

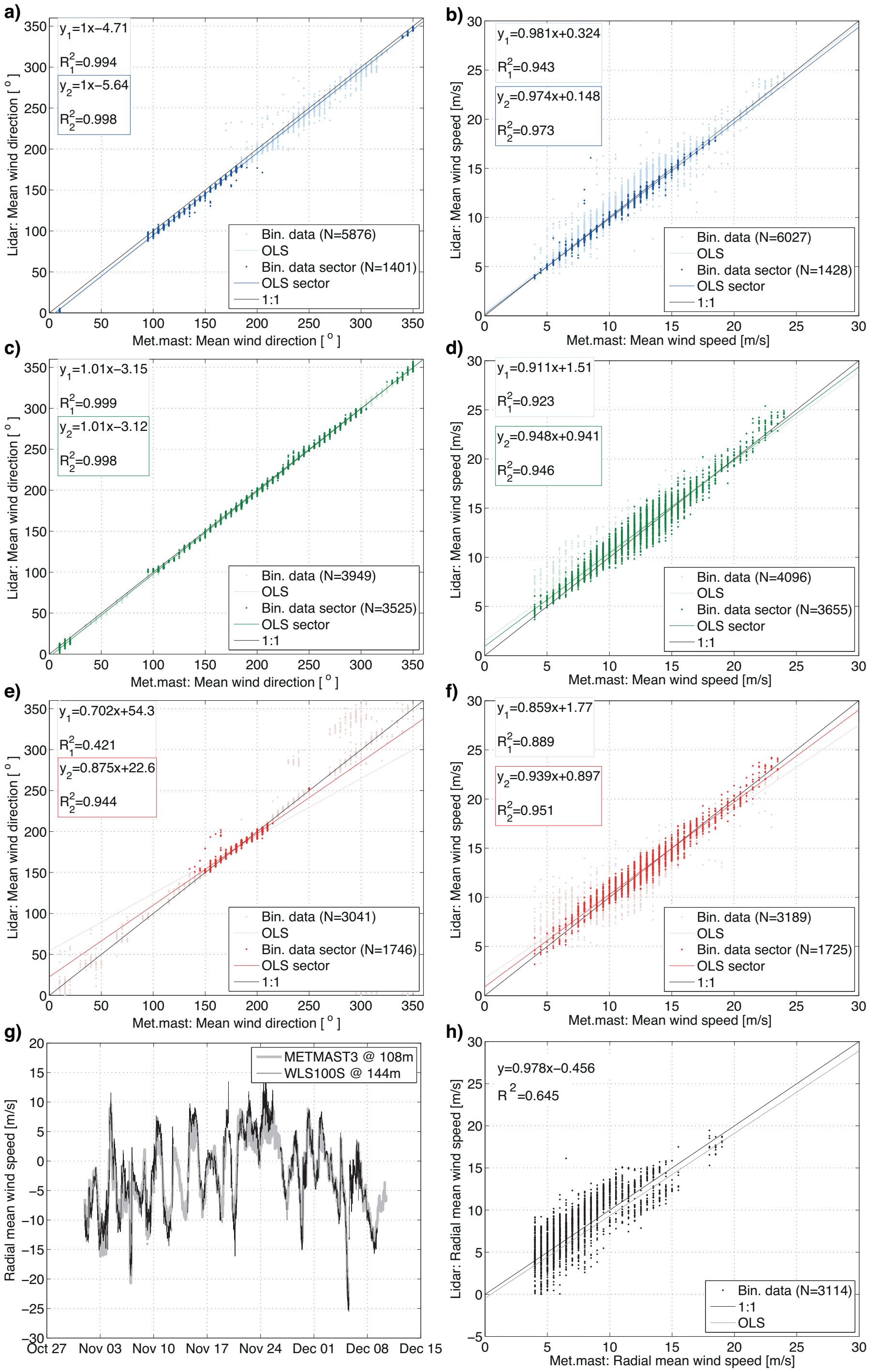

Fig. 3. a) to f) Scatter plots of 10 minutes mean wind direction (left) and horizontal wind speed (right) measured by a sonic anemometer and Windcubes V1 at 108 m height. Blue, green and red colors indicate the different Windcubes WLS67, WLS65 and WLS37 respectively. Disturbed wind directions are more transparent and solid lines indicate the 1:1 diagonal and the ordinary least square fit of the binned data points.
g) and h) Time series and scatter plot of 10 minutes mean radial wind speeds measured by a sonic anemometer at 108 m (gray) and a Windcube 100s range gate at 144 m height (black).

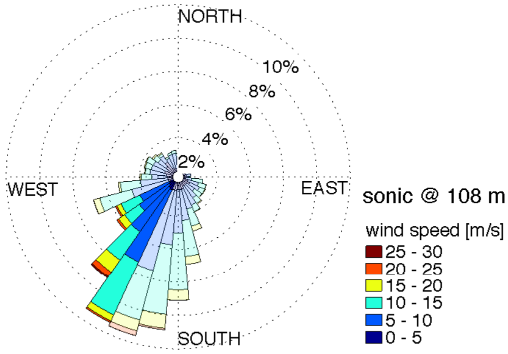

Fig. 4. Windrose of Sonic anemometer at 108 m height from November 2013 until March 10th 2014. The highlighted sector represents winds coming from the south-west (202.5° - 247.5°).

meandering effects vanish and the wake becomes a straight band of deficits still around 7 ms^{-1}. On a daily average the wake gets of a more conical shape with smooth deficits of 4 ms^{-1} in the near wake area and to 2 ms^{-1} in the far wake area (> 5D).

A high enough sampling rate allowed us to calculate the turbulence intensity of the radial velocities during a period of ten minutes. During ten minutes, turbulence intensities with 30% are highest at the flanks of the wake (figure 6). Signatures of the prototype turbine wakes are also visible in lines of TI with only a 10% smaller magnitude than the wakes of the research turbines. When averaging over a day, TI decays from 40% at 2D to 20% at 5D and forms a more uniform area. After 5D downstream distance of the turbine TI seams to decrease by another 10%. At this distance the height of the scanned line of sight is at 46 m and TI induced by the wake is of the same magnitude than the ambient air turbulence. Averaging over the whole analysed period for south-westerly winds makes the wake areas more symmetric compared to the daily mean picture.

Further analysis of all south-westerly winds measured by the three Windcubes V1 at three fixed positions show that wind profiles follow nicely the theoretical approach of an upstream logarithmic profile and downstream velocity deficits with increased turbulence intensities below blade tip height (figure 7). Velocity deficits range from 4 ms^{-1} to 1 ms^{-1} dependent on downstream distance and weather condition. The same applies to differences in TI, which vary between 10 and 22%. The wind speeds standard deviations are generally higher for the downstream devices which can be related to higher measurement uncertainties and the varying position inside the wake.

Filtering the data according to their stability class revealed highest TI values for stable weather conditions going along with highest velocity deficits for both downstream devices. Under these conditions the power output of the research turbine number 6 is lower than the average of the analysed period. During unstable cases the velocity deficit is smaller than in stable cases and the wake seems to almost recover at 5D downstream distance. Enhanced vertical mixing also expands the vertical extent of the wake and decreases the vertical wind shear. Under neutral conditions wake characteristics are weaker as TI and velocity deficits are smaller. Similar to the unstable conditions the velocity deficit is almost gone at 5D but TI is still 3% higher compared to upstream conditions. Weaker characteristics can be explained by stronger winds that introduce vertical mixing through vertical wind shear. The daily mean radial TI measured during unstable conditions by the Windcube 100s fits with 20 % at the location of the WLS7-37 and 10% at the location of the WLS7-65 well to their measured TI ranges.

5. Conclusion and Outlook

In this study we analysed static and scanning Windcube data collected during the WINd Turbine Wake EXperiment Wieringermeer (WINTWEX-W), in terms of wake characteristics. The data was collected from November 2013 until May 2014 in the collaboration with University of Bergen, CMR and the ECN.

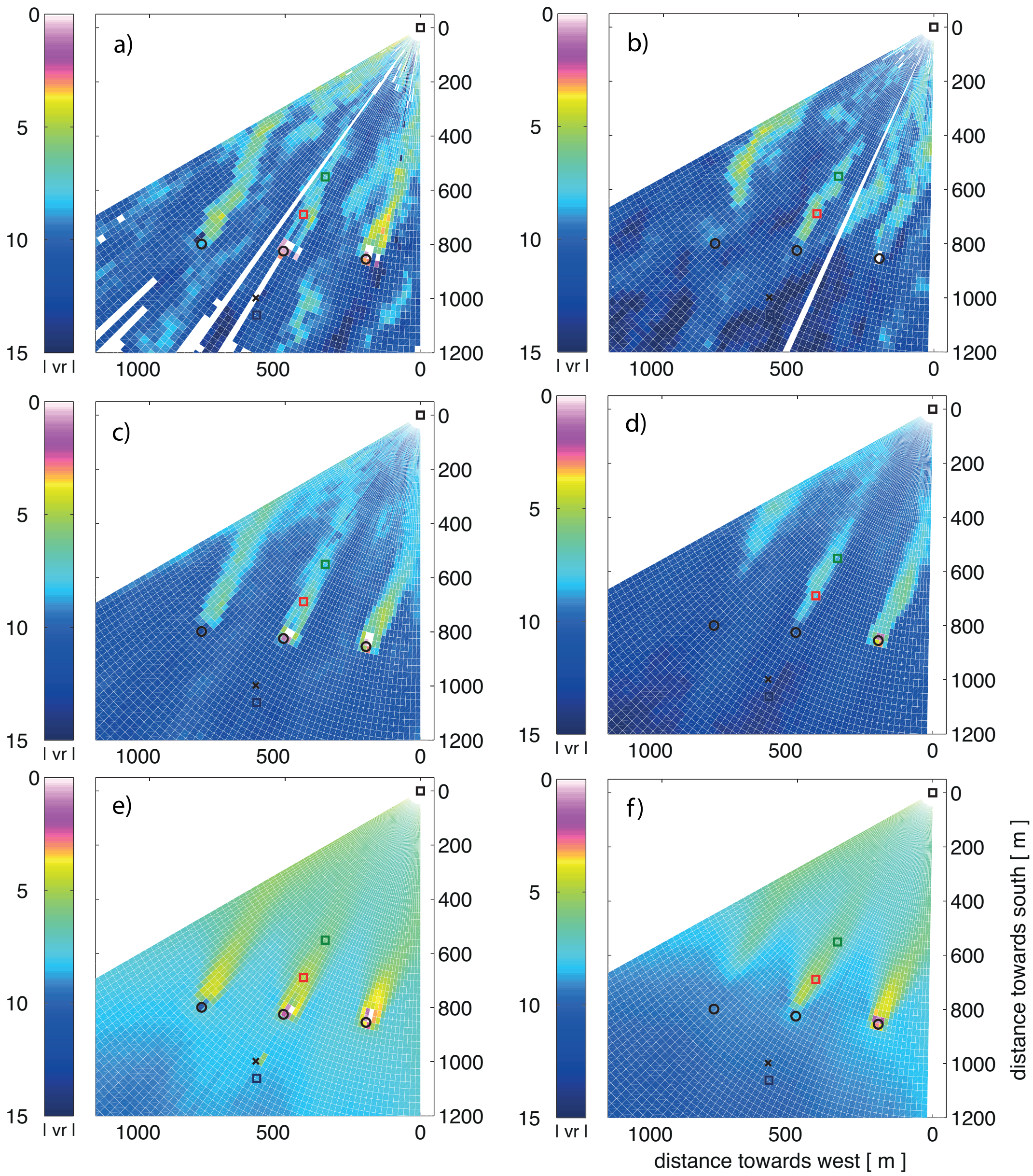

Fig. 5. Contour plots of 60° PPI scans at 4.7° (left) and 7.1° (right) elevation angle of a) & b) instantaneous, c) & d) 10 minutes mean and e) & f) daily mean radial wind speeds on November 1st, 2013. Circles, squares and the cross indication the locations of turbines, Windcubes and the met mast, respectively.

Windcube profile measurements show at neutral conditions a classical wake picture with a three month average flow deceleration and Turbulence Intensity of 3 ms^{-1} and 14% at two rotor diameter downstream distance. These four month averages are lower compared to results of the scanning Windcube 100S with deficits of 5 ms^{-1} and TI of 20%. The Windcube 100S results are consistent with wind tunnel and model studies ([29]). Differences to the static devices can be explained by the varying location of the measured profile inside the wake.

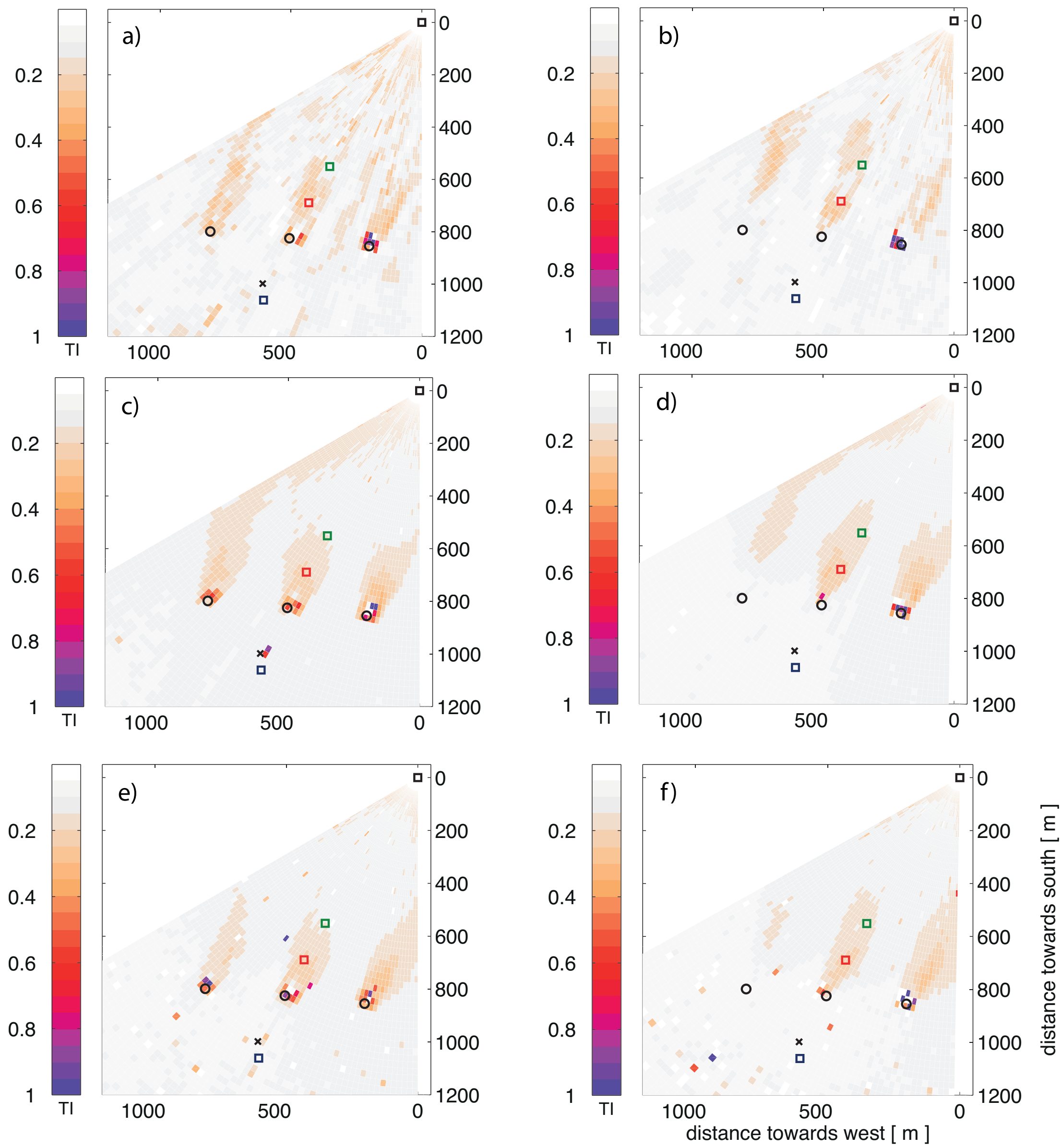

Fig. 6. Contour plots of 60° PPI scans at 4.7° (left) and 7.1° (right) elevation angle of turbulence intensity of a) & b) 10 minutes, c) & d) one day on November 1st, 2013 and e) & f) the analysed period for south-westerly winds. Circles, squares and the cross indicate the locations of turbines, Windcubes and the met mast, respectively.

However, the Windcube v1 measurements have proven to be of valuable information although measurement errors of ≤ 1 ms^{-1} and a variation of the profile location are expected. A look at different atmospheric stability conditions reveal that turbulence intensities and velocity deficits are strongest during stable conditions, as negative temperature gradients prohibit mixing with the ambient flow. As the turbines are influence by the upstream prototype turbines they generate less energy in stable conditions. During unstable conditions turbulence intensities varying between 10 and

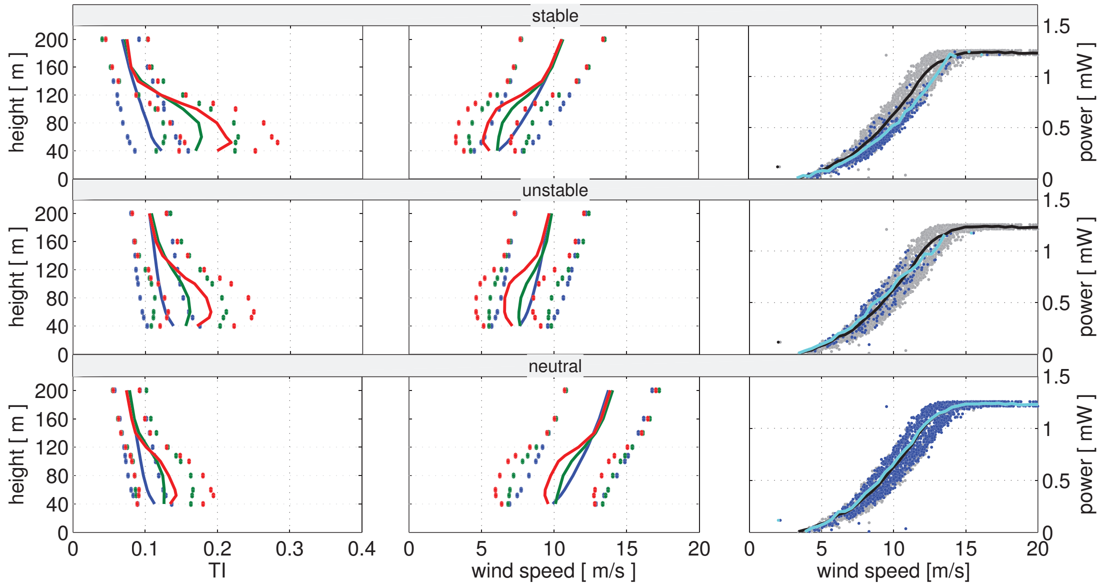

Fig. 7. Solid lines show Windcube V1 mean turbulence intensity and wind speed upstream (blue), near wake (red) and fare wake (green) profiles of the analysed period from November 2013 until mid March 2014 in the left and central column. Dots indicate the standard deviation. The right column shows 10 minutes mean and 0.5 ms^{-1} binned power output of turbine number 6 in dots and solid lines. Data belonging into the horizontally separated stability classes are highlighted in blue. Only data during south-westerly winds are shown.

19% and compare well to wind tunnel studies, while velocity deficits are not as strong as in the wind tunnel set up ([30]). Enhanced vertical mixing might be underestimated in the wind tunnel and is leading in our measurements to a greater vertical expansion of the wake. In the fare wake region the flow deficit has recovered almost to upstream conditions, but still has 3% higher turbulence intensities. High enough wind speed during neutral condition induce similar mixing effects as during unstable conditions.

In the future the data will be analysed in terms of spectral energy density to learn more about the turbulence input by the wind turbine dependent on different stability conditions. This information and the experienced gained by WINTWEX-W can be taken offshore as wake of upstream turbines could influence the natural frequencies of floating wind turbines.

References

[1] Chamorro, L.P., Porté-Agel, F.. Turbulent flow inside and above awind farm: A wind-tunnel study. Energies 2011;4:1916–1936. doi:10.3390/en4111916.

[2] Chamorro, L., Arndt, R.E.A., Sotiropoulos, F.. Turbulent Flow Properties Around a Staggered Wind Farm. Boundary-Layer Meteorology 2011;141(3):349–367. URL: http://dx.doi.org/10.1007/s10546-011-9649-6. doi:10.1007/s10546-011-9649-6.

[3] Hancock, P.E., Pascheke, F.. Wind-Tunnel Simulation of the Wake of a Large Wind Turbine in a Stable Boundary Layer: Part 2, the Wake Flow. Boundary-Layer Meteorology 2014;151(1):23–37. URL: http://dx.doi.org/10.1007/s10546-013-9887-x http://link.springer.com/10.1007/s10546-013-9887-x. doi:10.1007/s10546-013-9887-x.

[4] Krogstad, P.A.g., Sæ tran, L., Adaramola, M.S.. Blind Test 3 calculations of the performance and wake development behind two in-line and offset model wind turbines. Journal of Fluids and Structures 2014;URL: http://linkinghub.elsevier.com/retrieve/pii/S0889974614002175. doi:10.1016/j.jfluidstructs.2014.10.002.

[5] Mehta, D., van Zuijlen, A., Koren, B., Holierhoek, J., Bijl, H.. Large Eddy Simulation of wind farm aerodynamics: A review. Journal of Wind Engineering and Industrial Aerodynamics 2014;133:1–17. URL: http://linkinghub.elsevier.com/retrieve/pii/S0167610514001391. doi:10.1016/j.jweia.2014.07.002.

[6] Zhang, W., Markfort, C.D., Porté-Agel, F.. Near-wake flow structure downwind of a wind turbine in a turbulent boundary layer. Experiments in Fluids 2011;52(5):1219–1235. URL: http://link.springer.com/10.1007/s00348-011-1250-8. doi:10.1007/s00348-011-1250-8.

[7] Wu, Y.T., Porté-Agel, F.. Simulation of Turbulent Flow Inside and Above Wind Farms: Model Validation and Layout Effects. Boundary-Layer Meteorology 2013;146(2):181–205. URL: http://dx.doi.org/10.1007/s10546-012-9757-y http://link.springer.com/10.1007/s10546-012-9757-y. doi:10.1007/s10546-012-9757-y.

[8] Sanderse, B., Pijl, S., Koren, B.. Review of computational fluid dynamics for wind turbine wake aerodynamics. Wind Energy 2011;14(7):799–819. URL: http://doi.wiley.com/10.1002/we.458. doi:10.1002/we.458.

[9] Peña, A., Rathmann, O.. Atmospheric stability-dependent infinite wind-farm models and the wake-decay coefficient. Wind Energy 2014;17(8):1269–1285. URL: http://dx.doi.org/10.1002/we.1632 http://doi.wiley.com/10.1002/we.1632. doi:10.1002/we.1632.

[10] Abkar, M., Porté-Agel, F.. The effect of free-atmosphere stratification on boundary-layer flow and power output from very large wind farms. Energies 2013;6:2338–2361. doi:10.3390/en6052338.

[11] Sathe, A., Mann, J., Barlas, T., Bierbooms, W., van Bussel, G.. Influence of atmospheric stability on wind turbine loads. Wind Energy 2013;16(7):1013–1032. URL: http://dx.doi.org/10.1002/we.1528 http://doi.wiley.com/10.1002/we.1528. doi:10.1002/we.1528.

[12] Friedrich, K., Lundquist, J.K., Aitken, M., Kalina, E.A., Marshall, R.F.. Stability and turbulence in the atmospheric boundary layer: A comparison of remote sensing and tower observations. Geophysical Research Letters 2012;39(3):n/a–n/a. URL: http://dx.doi.org/10.1029/2011GL050413 http://doi.wiley.com/10.1029/2011GL050413. doi:10.1029/2011GL050413.

[13] Wharton, S., Lundquist, J.K.. Atmospheric stability affects wind turbine power collection. Environmental Research Letters 2012;7(1):14005. URL: http://stacks.iop.org/1748-9326/7/i=1/a=014005 http://stacks.iop.org/1748-9326/7/i=1/a=014005?key=crossref.df26a50fc7064a0a7c4f98db89353d29. doi:10.1088/1748-9326/7/1/014005.

[14] Barthelmie, R.J., Larsen, G.C., Frandsen, S.T., Folkerts, L., Rados, K., Pryor, S.C., et al. Comparison of Wake Model Simulations with Offshore Wind Turbine Wake Profiles Measured by Sodar. Journal of Atmospheric and Oceanic Technology 2006;23(7):888–901. URL: http://dx.doi.org/10.1175/JTECH1886.1. doi:10.1175/jtech1886.1.

[15] Trombe, P.J., Pinson, P., Vincent, C., Bø vith, T., Cutululis, N.A., Draxl, C., et al. Weather radars - the new eyes for offshore wind farms? Wind Energy 2013;:n/a–n/aURL: http://dx.doi.org/10.1002/we.1659 http://doi.wiley.com/10.1002/we.1659. doi:10.1002/we.1659.

[16] Gottschall, J., Courtney, M.S., Wagner, R., Jø rgensen, H.E., Antoniou, I.. Lidar profilers in the context of wind energy-a verification procedure for traceable measurements. Wind Energy 2012;15(1):147–159. URL: http://doi.wiley.com/10.1002/we.518. doi:10.1002/we.518.

[17] Kumer, V.M.. Analysis of Lidar Wind Measurements at the Bruck an der Leitha Wind Park. Master thesis; Universit{ä}t Wien; Institut f{ü}r Meteorologie und Geophysik UZA II, Althanstra{ß}e 14, 1090 Wien; 2012.

[18] Mann, J., Cariou, J.P., Courtney, M.S., Parmentier, R., Mikkelsen, T., Wagner, R., et al. Comparison of 3D turbulence measurements using three staring wind lidars and a sonic anemometer. Meteorologische Zeitschrift 2009;18(2):135–140. URL: http://openurl.ingenta.com/content/xref?genre=article&issn=0941-2948&volume=18&issue=2&spage=135. doi:10.1127/0941-2948/2009/0370.

[19] Sathe, A., Mann, J.. A review of turbulence measurements using ground-based wind lidars. Atmospheric Measurement Techniques 2013;6(11):3147–3167. URL: http://www.atmos-meas-tech.net/6/3147/2013/. doi:10.5194/amt-6-3147-2013.

[20] Iungo, G.V., Porté-Agel, F.. Measurement procedures for characterization of wind turbine wakes with scanning Doppler wind LiDARs. Advances in Science and Research 2013;10:71–75. URL: http://www.adv-sci-res.net/10/71/2013/. doi:10.5194/asr-10-71-2013.

[21] Iungo, G.V., Porté-Agel, F.. Volumetric LiDAR scanning of wind turbine wakes under convective and neutral atmospheric stability regimes. Journal of Atmospheric and Oceanic Technology 2014;:140822100122000URL: http://journals.ametsoc.org/doi/abs/10.1175/JTECH-D-13-00252.1. doi:10.1175/JTECH-D-13-00252.1.

[22] Käsler, Y., Rahm, S., Simmet, R., Kühn, M.. Wake Measurements of a Multi-MW Wind Turbine with Coherent Long-Range Pulsed Doppler Wind Lidar. Journal of Atmospheric and Oceanic Technology 2010;27(9):1529–1532. URL: http://journals.ametsoc.org/doi/abs/10.1175/2010JTECHA1483.1. doi:10.1175/2010JTECHA1483.1.

[23] Trujillo, J.J., Bingöl, F., Larsen, G.C., Mann, J., Kühn, M.. Light detection and ranging measurements of wake dynamics. Part II: two-dimensional scanning. Wind Energy 2011;14(1):61–75. URL: http://onlinelibrary.wiley.com/doi/10.1002/we.402/full http://doi.wiley.com/10.1002/we.402. doi:10.1002/we.402.

[24] Clifton, A., Elliott, D., Courtney, M.. RECOMMENDED PRACTICES FOR REMOTE SENSING FOR WIND ENERGY APPLICATIONS. IEA wind 2012;.

[25] M. Courtney, R. Wagner, T. Frils Pedersen, M. Bardon, S.D.. Calibrating Nacelle Lidars. January; 2012. ISBN 9788792896292.

[26] Hu, B.. Wind speed and wake studies using scanning LiDAR measurements. Tech. Rep. February; 2015.

[27] Lundquist, J.K., Churchfield, M.J., Lee, S., Clifton, a.. Quantifying error of lidar and sodar Doppler beam swinging measurements of wind turbine wakes using computational fluid dynamics. Atmospheric Measurement Techniques 2015;8:907–920. URL: http://www.atmos-meas-tech.net/8/907/2015/. doi:10.5194/amt-8-907-2015.

[28] Rhodes, M.E., Lundquist, J.K.. The Effect of Wind-Turbine Wakes on Summertime US Midwest Atmospheric Wind Profiles as Observed with Ground-Based Doppler Lidar. Boundary-Layer Meteorology 2013;149:85–103. doi:10.1007/s10546-013-9834-x.

[29] Troldborg, N., Sø rensen, J.. A simple atmospheric boundary layer model applied to large eddy simulations of wind turbine wakes. Wind Energy 2014;17(August 2010):657–669. URL: http://onlinelibrary.wiley.com/doi/10.1002/we.1608/full. doi:10.1002/we.

[30] Zhang, W., Markfort, C.D., Porté-Agel, F.. Wind-Turbine Wakes in a Convective Boundary Layer: A Wind-Tunnel Study. Boundary-Layer Meteorology 2013;146(2):161–179. URL: http://link.springer.com/10.1007/s10546-012-9751-4. doi:10.1007/s10546-012-9751-4.